Time and spatially resolved spectroscopic measurement of temperatures in a free-burning arc by monochromatic imaging (published, see [1])

Shuiliang Ma, Hongming Gao, Lin Wu, and Senmu Zheng

State Key Laboratory of Advanced Welding Production Technology, Harbin Institute of Technology, Harbin 150001, China

Abstract

An imaging method that involves a high-speed camera and a narrow-band filter has been used to acquire images of the argon atomic line intensity of a free-burning arc plasma at atmospheric pressure. The measured lateral intensities are converted to radially distributed emission coefficients by means of an Abel inversion. Under the assumption of local thermodynamic equilibrium, the time resolved temperature distributions in the arc have been determined. Both the intensities and temperatures indicate that the arc was gradually evolving towards a static state after it was ignited; the temperature at any position of the arc column shows the same decreasing trend. These results demonstrate that this method enables the time and spatially resolved properties of plasmas to be characterized and thus it may bring new findings and applications concerning the diagnostics of plasmas.

1. Introduction

Arc plasmas have widely been used in industrial areas of welding, cutting, spraying and surface modification [2]. In order to improve these applications, the properties of the plasma should be characterized. In particular, the spatial and temporal distributions of plasma parameters such as the electron temperature and density are of great interest to many fields of physics and engineering [3,4], as they can provide important insight into the basic processes that occur in the plasma. For the determination of these parameters, optical emission spectroscopy as a non-invasive diagnostic method has been adopted in most cases. Since the plasma is characterized with small volume and large gradients of some quantity, a spatially resolved measurement of the distribution of the light emitted from the source is needed.

Over the past few decades, a point-by-point scanning with a spectrograph has extensively been used to collect the spectra of plasmas [5–8]. This method is relatively simple, accurate and inexpensive, but is lack of spatial resolution, thus the time required to complete the measurement is long. Long acquisition times require the arc to be steady enough in the measurement and prohibit the investigation of transient phenomena, such as plasma fluctuation and evolution.

For time and spatially resolved measurements of plasma intensities, monochromatic imaging is a more efficient approach and has been attracted great interest in recent years. One method uses a monochromator to obtain two dimensional images. Its utilization is extensive, such as inspecting aluminum vapor in a helium vacuum arc [9] and measuring the distribution of excited species in a radio frequency (RF) plasma [10]. Another method using narrow-band filters in conjunction with two-dimensional imaging detectors, which is relatively simple and has a very short acquisition time, is also widely used. The radiation flux emitted by an argon plasma jet at atmospheric pressure was characterized by this method [11]. The cause of the enhanced glow in the void of the dust particle cloud was revealed by line ratio imaging of two spectral lines with two synchronized cameras [12]. Such a line ratio imaging method was also used to determine the temperature and metal vapor concentration in a copper breaking arc [13].

Recently, the group in our laboratory has been using the imaging method to measure the temperature and electron density distributions of free-burning argon arcs at atmospheric pressure. Both the continuum radiation [14] and spectral line intensity [15] were used and good results have been obtained. The imaging method has proved to be a reliable and suitable method for the diagnostics of arc plasmas.

In arc plasma welding, defects most possibly occur when the arc is ignited. It is therefore important to understand the time resolved behavior of the plasma. But till now most work [5–8] has been concerned with the static arc based on a spectrograph scanning measurement, the properties of the arc after ignition have not yet been investigated. In this work we describe the application of the imaging method in observing the evolution of a free-burning argon arc at atmospheric pressure. The spatial and temporal distribution of the ArI 794.8 nm spectral line intensity in the arc is detected by a high-speed camera by using a narrow-band filter. Since the amount of the images acquired by this system is very large, an efficient Abel inversion method is programmed to reconstruct the radial emission coefficients from the measured lateral intensities. Then the time variation of the arc temperature is derived from the emission coefficients.

2. Experimental details

The experimental set-up is shown schematically in figure 1. A common tungsten inert gas (TIG) welding torch and a direct current power source were used to generate the arc. The gas shielding nozzle of the torch had an internal diameter of 10 mm. Argon was used as the shielding gas with a flow rate of 10 L/min. The arc was struck and burned free at atmospheric pressure between a tungsten cathode and a copper plate anode. The cathode electrode was a 2.4 mm diameter, thoriated tungsten rod ground to a conical tip with an included angle 60°. The anode was water-cooled to ensure the copper without melting and keep the arc steady in the measurement. The distance between the cathode tip and the copper plate was 5 mm. An arc current of 200 A was used.

Arc images were acquired by using an imaging system that consists of lenses, neutral density and narrow-band filters and a detector. Light from the arc was imaged and collimated before passing through the filters to the detector. The imaging lens L_1 was placed far away from the arc source to ensure the parallel-ray projection condition was approximately satisfied, as assumed in the Abel inversion process. Lens L_1 can be moved forward and backward, so the magnification of the image on the detector can be adjusted according to the experimental conditions. After collimation by lens L_2, the light was perpendicularly projected to the neutral density and narrow-band filters and focused at the image plane of the detector by lens L_3. Such a design ensures that the central wavelength of the narrow-band filter is not shifted, and thus the interested spectral line can be acquired accurately. The detector is a Dalsa CA-

Email: shlgma@126.com (Shuiliang Ma).

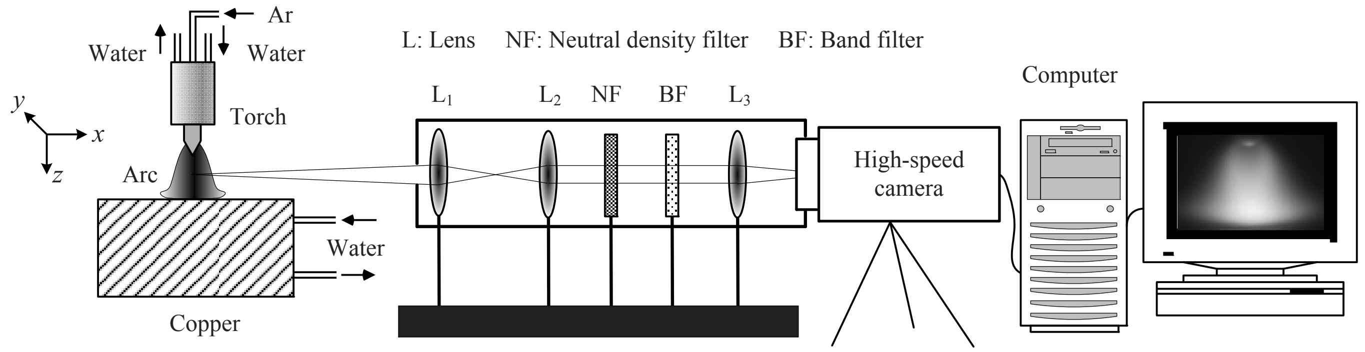

Fig. 1. Schematic diagram of the experimental set-up.

D6-0256W high-speed camera, which is capable of acquiring 8-bit grey images at a frame rate up to 955 Hz and at a spatial resolution of 260×260 pixels corresponding to the sensor size of 2.6×2.6 mm. Since the radiation from the arc is so strong that a neutral density filter must be placed in the front of the narrow-band filter. In this case, with the aperture of the camera being carefully tuned, images of high intensity, but free from the effects of saturation can be obtained.

From a spectroscopic measurement we found that the ArII spectral lines only appeared in the high-temperature area, i.e., the column near the cathode of the arc, while the ArI spectral lines appeared in any position of the arc. Therefore, the ArI 794.8 nm line was selected for the determination of the arc temperatures. The reason we chose this line is that it is well separated from other lines and the line intensity is not weak. The narrow-band filter centred at wavelength 794.8 nm and with a full width at half maximum of 3.1 nm was used to acquire the line intensity distributions. Figure 2 shows the transmittance curve of the filter. The spectra of the arc that passed through the filter were recorded by using a spectroscopic analysis system; no other spectral line was found except for the interested one. Since the influence of other spectral lines was completely avoided, the performance of the selected filter is reliable. The acquired image consists of only the intensity of the ArI 794.8 nm line and the continuum radiation near the same wavelength.

3. Data processing and measurement

Since the measurements are line-of-sight integrated intensities, for the determination of plasma parameters such as the particle temperature and density, the distribution of emission coefficients must be reconstructed. This is accomplished by means of an Abel inversion, provided the plasma is cylindrically symmetric and optically thin. But due to fluctuations in the plasma and the noise introduced when acquiring images, the experimentally measured intensities are not completely symmetric. Even a slight asymmetry of the intensity profile will greatly affect the accuracy of the inversion [16]. Therefore, a symmetrization procedure was implemented before Abel inversion.

The symmetrization process has two steps. First, the symmetric center of the intensity curve is determined and shifted to the center of the data sequence; then, the data points at both sides of the center are averaged to yield a symmetric distribution. The symmetric center was determined using the method based on the possibility statistics of noise in the measured data [17]. Other methods, such as assuming the center at the half distance between two points at both sides of the intensity profile with a same height, are not considered as they are less accurate.

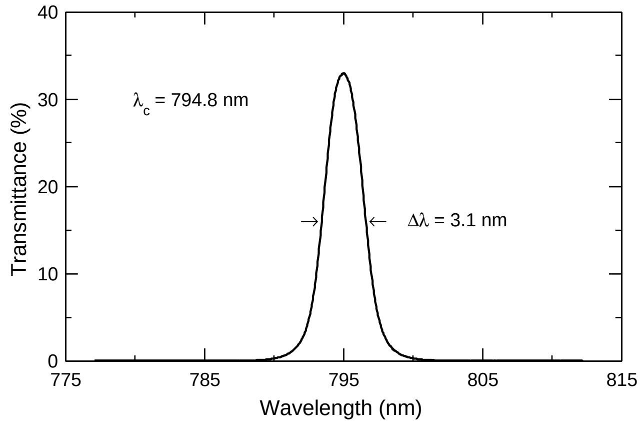

Fig. 2. Transmittance curve of the narrow-band filter.

Interpolation process is not necessary as the intensity data collected with the camera already have a high spatial resolution.

Radially distributed emission coefficients were reconstructed from the symmetrized intensity data by Abel inversion using the versatile polynomial fitting [18] or modified Fourier-Hankel [19] method. These methods are not sensitive to noise and can yield more accurate results than other inversion algorithms, especially for small sets of data. For the modified Fourier-Hankel method, the relation between the intensity $I(y)$ and the emission coefficient $\varepsilon(r)$ can be described as

$$\varepsilon(r_i) = \frac{\alpha^2\pi}{2nR} \sum_{j=-n}^{n-1} I(y_j) \sum_{k=1}^{\lfloor n/\alpha \rfloor} k\, J_0\Big(\frac{\alpha ik\pi}{n}\Big) \cos\Big(\frac{\alpha jk\pi}{n}\Big),$$

where R is the radius of the plasma source, n is the number of data points at one side of the source, $r_i = iR/n$, $y_j = jR/n$, and α is a factor which should satisfy $0 < \alpha \leq 1$. Since the inversion method was presented in a matrix form, the processing speed is very fast even for large amounts of data. The method is thus very suitable for processing of the images acquired with the imaging system.

The arc temperatures were determined by using the Fowler-Milne method, which is also known as the normal temperature method [5–7]. This method does not require absolute intensity calibration and the knowledge of atomic transition probabilities, thus precise values of temperature can be derived from reconstructed radial emission coefficients. The only restriction is that the plasma investigated should be in local thermodynamic equilibrium and the radial distribution of the emission coefficients should have an off-axis maximum.

4. Results and discussion

Figure 3 shows the images of the ArI 794.8 nm line of a 200-A free-burning arc acquired for two different time delays,

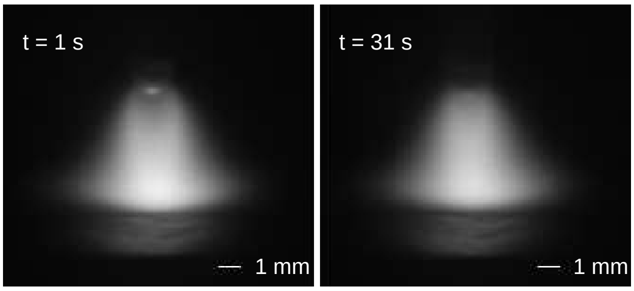

Fig. 3. Two monochromatic images of the ArI 794.8 nm line acquired after the arc was ignited with time delays of $t = 1$ and 31 s. The distance from the arc cathode tip to the anode was 5 mm, and the arc current was 200 A.

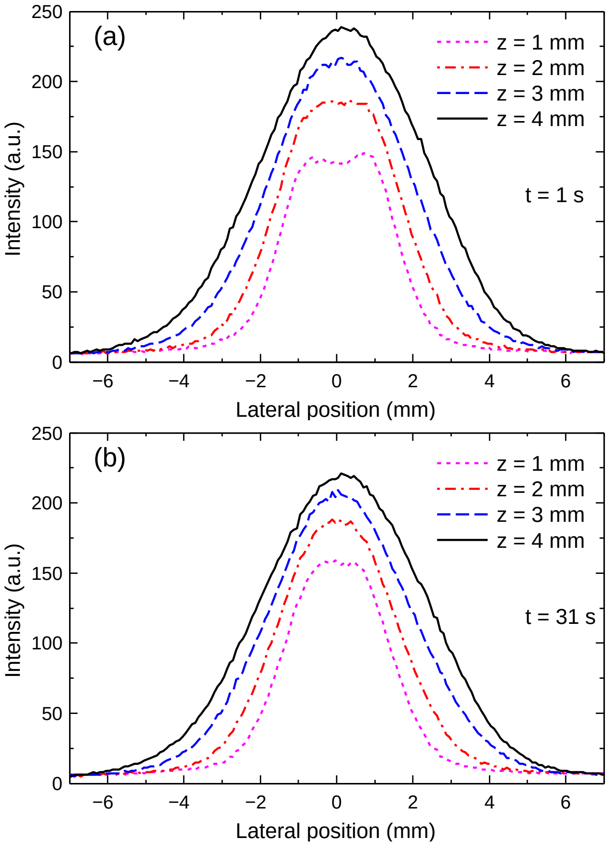

Fig. 4. Intensity distributions at various layers of the arc for the two images shown in figure 3: (a) $t = 1$ s; (b) $t = 31$ s. The layers are with distances from the arc cathode tip of 1, 2, 3, and 4 mm.

$t = 1$ and 31 s. In order to reduce the background and improve the signal-to-noise ratio, the exposure time was set less than 1 ms. This exposure time corresponds to the highest image acquiring speed of the camera. Under such condition, images at a time period of about 5 s can be obtained continuously. Time larger than 5 s is possible by increasing the computer memory. The image for $t = 1$ s was one frame of a run that was performed as soon as the cooling water both for the torch and the copper plate anode started and the arc was ignited. The image for $t = 31$ s was one frame of another run, which began after the arc was burning 30 s.

The difference between the two images shown in figure 3 can easily be distinguished; the intensity in the cathode area of the arc for $t = 1$ s is lower than that of the second image. In order to show the difference more clearly, the intensity distributions at different layers of the images are presented in figure 4. The intensity curve for $t = 1$ s and $z = 1$ mm (the distance from the arc cathode tip) shows an off-axis maximum at a lateral position about 1 mm, while the intensity distribution for $t = 31$ s and $z = 1$ mm does not have such a characteristic. At the anode arc column ($z \geq 3$ mm), where the arc temperature is much lower, both intensity curves at $t = 1$ and 31 s are bell-shaped; the only difference is that the intensity at $t = 31$ s decreased. Such differences indicate that the arc was not in a static state; it was evolving with time after it was ignited.

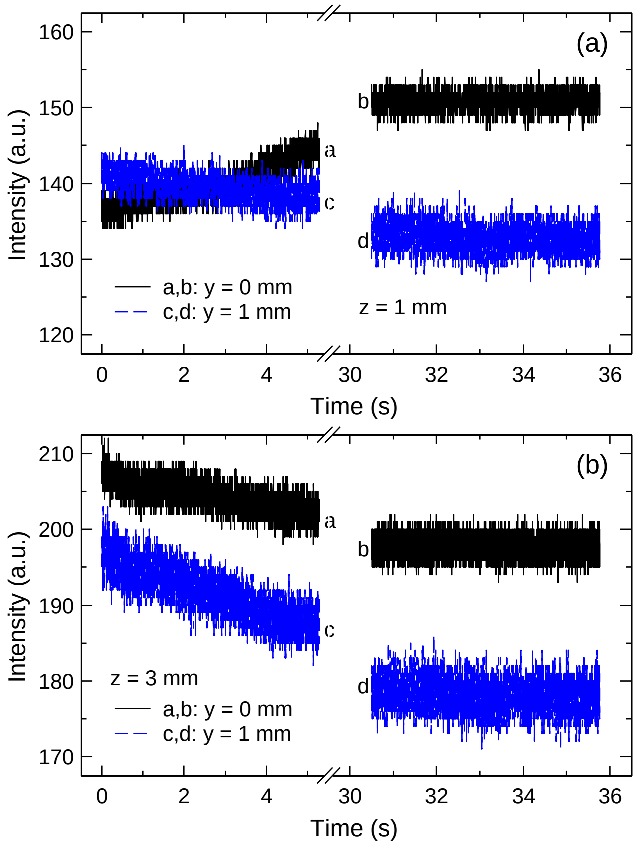

Fig. 5. Time variation of measured spectral line intensities at different positions of a 200 A free-burning arc: (a) $z = 1$ mm; (b) $z = 3$ mm.

Figure 5 shows the time variation of the intensities at two axial positions of the arc. These curves evidently show that the arc was gradually evolving to a static state in a few seconds. In figure 5 (a) the intensities at two lateral positions $y = 0$ and 1 mm are compared. It is interesting to note that the intensities at these positions varied oppositely for $t < 30$ s. An off-axis maximum appears in the lateral intensity distribution when the value at position $y = 0$ mm is lower than that at position $y = 1$ mm (see the profile for $z = 1$ mm in figure 4 (a)). It is thus clear that the intensity profile in the arc for $z = 1$ mm varied from the off-axis peak type to the bell-shaped type after a few seconds. An off-axis type curve is always associated with a higher arc temperature. Therefore, the evolution of the intensities implies that the local temperature of the arc decreases with time. The intensities presented in figure 5 (b) for positions $y = 0$ and 1 mm show a decreasing trend. This is because the intensity curves in this cross section of the arc do not belong to the off-axis peak type; they are bell-shaped. From the decreasing tendency we can also conclude that the arc temperature drops as time goes on.

From the measured lateral intensities the radially resolved emission coefficients at different axial positions of the arc were obtained by means of an Abel inversion. Then using the Fowler-Milne method, frame by frame, the temperature distributions of the arc at different times were calculated. Figure 6 shows the temperatures at three positions of the arc as functions of time. From these curves we can see that the temperature of the free-

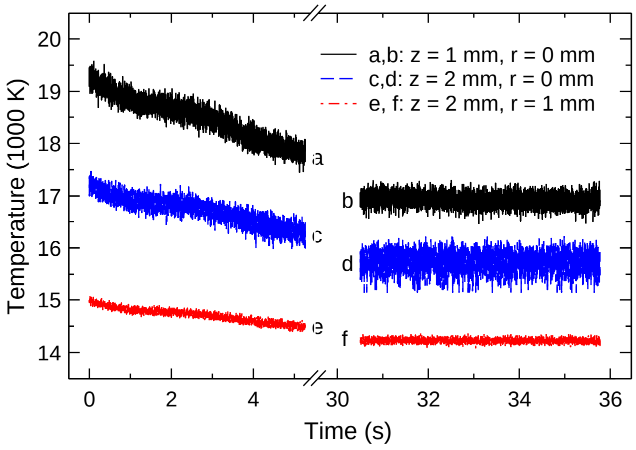

Fig. 6. Time variation of calculated temperatures at different positions of a 200 A free-burning arc at atmospheric pressure.

burning arc indeed decreased gradually before the arc reached thermal equilibrium. In contrast to the intensities presented in figure 5, the temperature at any position of the arc shows the same decreasing trend. The arc evolution tendency can be more accurately reflected from the temperature variation. The temperature decreasing trend may arise from many factors. To find the cause will be valuable for understanding the processes that occur within the plasma and thus can provide information for the monitoring and control of welding processes.

From figure 6 we can also see that the error in the temperatures caused by the fluctuations of the arc is less than 800 K; at positions far away from the axis, the error is even smaller. The higher central error is due to the property of Abel inversion, which is always much difficult to yield an accurate result near the axis. The uncertainty in the temperature indicates that the accuracy of the imaging method is quite satisfied; the maximum uncertainty is less than 4%. If the time resolution is not very important, the calculated temperatures can be averaged by a few frames. In this way the error can be reduced further.

It should be noted that, due to the continuum radiation which cannot be subtracted from the measured line intensities, the calculated temperature will be a little lower[15], especially for temperatures higher than 17 000 K. To avoid this problem, in future studies we plan to design a new imaging system which can simultaneously measure the distributions of the line intensity and the continuum radiation of the arc.

5. Conclusion

An imaging method has been used to study the evolution of a free-burning argon arc at atmospheric pressure. A high-speed camera in conjunction with a narrow-band filter is used to detect the spatially distributed intensities of the argon arc. From these measured intensities, the radial emission coefficient is reconstructed by means of an Abel inversion, and then the temperature distribution is determined. Both the time and spatially resolved intensity and temperature indicate that the arc was gradually evolving towards a static state after it was ignited; but the time variation of the temperature at any position of the arc displays the same decreasing trend. In addition, the uncertainty in the determined temperature is estimated to be less than 4%, which can be reduced further by averaging the temperature in a few frames. These results demonstrate that imaging is a powerful tool for the diagnostics of arc plasmas. This method is simple, fast and efficient; it may be used for the determination of temperatures either in static or dynamic plasmas, or for the monitoring and control of parameters in industrial plasma devices.

References

[1] S. Ma, H. Gao, L. Wu, S. Zheng, Time and spatially resolved spectroscopic measurement of temperatures in a free-burning arc by monochromatic imaging, Meas. Sci. Technol. 19 (10) (2008) 105602.
[2] U. Kogelschatz, Atmospheric-pressure plasma technology, Plasma Phys. Control. Fusion 46 (12) (2004) 63B–75B.
[3] J. Hlína, J. Gruber, J. Šonský, Application of a CCD camera to investigations of oscillations in a thermal plasma jet, Meas. Sci. Technol. 17 (4) (2006) 918–922.
[4] D. Doria, K. D. Kavanagh, J. T. Costello, H. Luna, Plasma parametrization by analysis of time-resolved laser plasma image spectra, Meas. Sci. Technol. 17 (4) (2006) 670–674.
[5] H. N. Olsen, The electric arc as a light source for quantitative spectroscopy, J. Quant. Spectrosc. Radiat. Transfer 3 (4) (1963) 305–333.
[6] G. N. Haddad, A. J. D. Farmer, Temperature measurements in gas tungsten arcs, Weld. J. 64 (12) (1985) 339s–342s.
[7] A. B. Murphy, Modified Fowler-Milne method for the spectroscopic measurement of temperature and composition of multielement thermal plasmas, Rev. Sci. Instrum. 65 (11) (1994) 3423–3427.
[8] J. Haidar, A. J. D. Farmer, Large effect of cathode shape on plasma temperature in high-current free-burning arcs, J. Phys. D: Appl. Phys. 27 (1994) 555–560.
[9] U. Kinrot, S. Goldsmith, R. L. Boxman, Monochromatic imaging of cathodic arc plasma, IEEE Trans. Plasma Sci. 24 (1) (1996) 71–72.
[10] W. A. Hareland, R. J. Buss, Distribution of excited species in plasmas by monochromatic imaging, IEEE Trans. Plasma Sci. 24 (1) (1996) 117–118.
[11] J. Dgheim, Charaterization of an argon plasma jet by the imagery method, Meas. Sci. Technol. 16 (8) (2005) 1650–1655.
[12] D. Samsonov, J. Goree, Line ratio imaging of a gas discharge, IEEE Trans. Plasma Sci. 27 (1) (1999) 76–77.
[13] M. Takeuchi, T. Kubono, Temperature and metal vapor near the cathode in copper breaking arcs according to spectroscopic measurement, IEEE Trans. Plasma Sci. 28 (3) (2000) 991–999.
[14] C. Xu, H. Gao, L. Wu, Application of monochromatic image method in arc plasma diagnostics, IEEE Trans. Plasma Sci. 33 (2) (2005) 304–305.
[15] S. Ma, H. Gao, L. Wu, Spatial spectroscopic diagnostics of arc plasmas by monochromatic imaging, IEEE Trans. Plasma Sci. ?? (9) (2008) 1350–1357.
[16] S. Nakamura, Estimating measurement error values resulting from the peak position error, when using the Abel inversion and the numerical method in argon inductively coupled plasma diagnostics, Spectrochim. Acta B 54 (1999) 1899–1902.
[17] L. M. Smith, D. R. Keefer, S. I. Sudharsanan, Abel inversion using transform techniques, J. Quant. Spectrosc. Radiat. Transfer 39 (1988) 367–373.
[18] S. Ma, H. Gao, G. Zhang, L. Wu, A versatile analytical expression for the inverse Abel transform applied to experimental data with noise, Appl. Spectro. ?? (9) (2008) 1350–1357.
[19] S. Ma, H. Gao, L. Wu, Modified Fourier-Hankel method based on analysis of errors in Abel inversion using Fourier transform techniques, Appl. Opt. 47 (9) (2008) 1350–1357.